Environmental Pollution 242 (2018) 264–276

Contents lists available at ScienceDirect

Environmental Pollution

journal homepage: www.elsevier.com/locate/envpol

Long term metal release and acid generation in abandoned mine wastes containing metal-sulphides☆

N. Eugenia Nieva, Laura Borgnino, M. Gabriela García*

Centro de Investigaciones en Ciencias de la Tierra (CICTERRA), CONICET, and FCEFyN Universidad Nacional de Córdoba, Córdoba, Argentina, Avda Velez Sarsfield 1611, 5016, Ciudad Universitaria, Córdoba, Argentina

ARTICLE INFO

Article history:
Received 10 April 2018
Received in revised form
24 May 2018
Accepted 21 June 2018
Available online 28 June 2018

Keywords:
Central andes
Acid mine drainage
Static tests
Sequential extractions
Metal release

ABSTRACT

The sulphide-rich mine wastes accumulated in tailing dumps of La Concordia Mine (Puna of Argentina) have been exposed to the weathering action for more than 30 years. Since then, a series of redox reactions have triggered the generation of a highly acidic drainage -rich in dissolved metals-that drains into the La Concordia creek. The extent of metal and acid release in the site was analysed through field surveys and laboratory experiments. Static tests were conducted in order to predict the potential of the sulphidic wastes to produce acid, while Cu-, Zn-, Fe- and Pb-bearing phases present in the wastes were identified by XRD, SEM/EDS analysis and sequential extraction procedures. Finally, the release of these metals during sediment-water interaction was assessed in batch experiments carried out in a period of nearly two years. Field surveys indicate that the prolonged alteration of the mine wastes led to elevated electrical conductivity, pH values lower than 4 and metal concentrations that exceed the guide values for drinking water in the La Concordia stream regardless of the dominating hydrological conditions. The highly soluble Fe and Mg (hydrous)sulphates that form salt crusts on the tailings surfaces and the riverbed sediments play an important role in the control of metal mobility, as they rapidly dissolve in contact with water releasing Fe, but also Cu and Zn which are scavenged by such minerals. Another important proportion of the analysed metals is adsorbed onto Fe (hydr)oxides or form less soluble hydroxysulfates. Metals present in these phases are released to water more slowly, thus representing a potential long term source of heavy metal pollution. The obtained results are a contribution to the understanding of long term metal transformations and mobility in mine waste-impacted sites.

© 2018 Elsevier Ltd. All rights reserved.

1. Introduction

The Puna region in Argentina (22° - 27° S) is a high plateau with altitudes that vary from 3500 to 4700 m a.s.l, which is exposed to a broad range of extreme climatic and environmental conditions such as aridity, large thermal amplitude, hypersalinity, acid hot springs and high levels of UV radiation. All these conditions determined that the region has been nearly isolated from direct human activity, with the exception of mining, which has been a local activity even before the Spanish colonization (Alonso, 2000). A number of small mines disseminated throughout the entire region produced copper, silver, lead and zinc from high sulphidation veins. Some of them have closed at the end of the twentieth century leaving their mine wastes exposed to the weathering action for decades. Although the environmental impact of mine wastes on the nearby ecosystems is well known, only a few comprehensive studies have been carried out in the region (e.g., Murray et al., 2014; Nieva et al., 2016). The occurrence of abandoned mine wastes derived from metal-sulphide prospects is not a local problem, but a regional environmental issue in the Andean region of Bolivia, Chile and Peru (e.g., Oblasser and Chaparro, 2008), as well as in many other regions of Argentina, such as in the central Andes (e.g., Chiavazza and Prieto, 2008), in the Pampean ranges (e.g., Lecomte et al., 2017) and in Patagonia (e.g., Idaszkin et al., 2017).

La Concordia mine is an ancient mine that produced Pb, Ag and Zn until 1986 when it closed. The mine wastes were abandoned in the site without treatment, and remain accumulated in four tailing dams constructed as a series of embankments along the narrow valley of the Concordia Creek and in piles disposed near the ancient mineral processing plant. The sediments accumulated in the tailing dams were affected by the progressive oxidation of the gangue

☆ This paper has been recommended for acceptance by Dr. Jorg Rinklebe.

* Corresponding author.
E-mail address: gabriela.garcia@unc.edu.ar (M.G. García).

https://doi.org/10.1016/j.envpol.2018.06.067
0269-7491/© 2018 Elsevier Ltd. All rights reserved.

sulphides (mostly pyrite and arsenopyrite), which resulted in the formation of weathering profiles characterized by a succession of layers that differ by color, consistency and textural features. The oxidation of pyrite is complex and involves a series of redox chemical and biological reactions that have been extensively described (e.g., Descostes et al., 2004; Druschel and Borda, 2006).

In a previous work, Nieva et al. (2016) determined that the oxidation of metal sulphides in La Concordia mine generated a highly acidic solution, rich in arsenic, dissolved metals and sulphate that drains into the creek and yields elevated concentrations of dissolved metals, high salinity and low pH values in the stretch impacted by the wastes. In addition, the intense evaporation triggers the precipitation of mineral salts in the form of saline crusts that cover the tailing's surface and the Concordia riverbed. These salts and some other oxidation by products such as Fe (hydr)oxides and hydroxysulphates may temporally scavenge dissolved metals and metalloids depending on the solubility of the host minerals or the type of bonding between the metals and the substrate. In the Concordia mine, the partitioning between the aqueous and solid phases has been specifically analysed for As, one of the most hazardous pollutants measured in the stream waters (i.e., Nieva et al., 2016). However the extent of the acid generation as well as the sources and dynamics of heavy metals have not been determined so far in the impacted site. Therefore, a detailed chemical and mineralogical characterization of these residues coupled with laboratory tests was carried out in order to determine the Cu, Zn, Fe and Pb phase associations as well as to evaluate the capacity for metal release over time of the mine wastes. In addition, the static tests ABA and NAG were conducted in order to determine their acid generating potential. Our goal is to assess the extent of acid generation as well as the sources and dynamics of heavy metals in sediments accumulated in the abandoned tailing dams in the Concordia mine. The obtained results are a contribution to the understanding of long term metal transformations and mobility in mine-impacted sites located in high altitude and arid environments.

2. Methodology

2.1. Study area

During the Middle Miocene, an important back-arc volcanism affected the Puna region (Matteini et al., 2002) and produced significant volcanic complexes and calderas associated with polymetallic mineralization (i.e., Oyarzun et al., 2000; Riller et al., 2001). This mineralization was typically hydrothermal and spatially and temporally associated with calco-alkaline magmatism (Hedenquist and Lowenstern, 1994).

The polymetallic hydrothermal mineralization that was under production in La Concordia mine, along with other mineral ores such as La Poma and El Queva, is associated with the volcanic complex of El Quevar (6130 m a.s.l., 24°18′31″S; 66°43′50″W). This epithermal deposit (high sulphidation) comprises two cycles of mineralization, the first one during the Upper Miocene age produced the Pb-Ag (Zn) mineralization and the second one during the Pliocene produced Sb-Au mineralization (Zappettini, 1990). The mining district was discontinuously mined since 1900 until the middle 1980′s, when it was definitively closed without executing appropriate practices of site remediation.

La Concordia mine is located in the Puna region of Salta province, NW Argentina (24°12′ S y 66° 24' W; 4200 m a.s.l.), 15 km NW the village of San Antonio de los Cobres (Fig. 1). The main geological and climatic characteristics of the study area have been described elsewhere (i.e., Nieva et al., 2016).

2.2. Field sampling and sample preparation

Mine wastes samples were collected in June 2014 from exposed weathering profiles in the tailings I and IV (Fig. 1). The sedimentological characteristics of these profiles are described in Nieva et al. (2016). Briefly, the depth profile in tailing I (Fig. 1a) consists of a ~200 cm depth succession of clayed silt and sandy layers, that have been divided into five layers. The two uppermost layers TI-A and TI-B are unsaturated and completely oxidized. A laterally discontinuous thin layer (TI-H) acts as a hardpan barrier that separates the uppermost unsaturated oxidized zone from the bottom sediments. Below the hardpan level, sediments in layers TI-C and TI-D are dark and show signs of predominantly reductive conditions. Only the bottom layer TI-D was completely saturated at the moment of sampling, while the layer TI-C showed some hydromorphic features that suggest periodic waterlogged conditions. Depth profile in tailing IV (Fig. 1b) consists of a ~210 cm depth succession of coarse to fine sands that were completely dry at the moment of sampling. Three layers (TIV-A, TIV-B, and TIV-C) were distinguished in this profile by their color, consistency and grain-size characteristics. Tailing IV was the first one built nearly 120 year ago. Since then, the accumulated sediments have suffered intense erosion and washing. Therefore, layer TIV-A represents the altered remnant portion of the original tailing, while layers TIV-B and TIV-C correspond to the red conglomerates of the Pirgua subgroup (Kirschbaum et al., 2012) that cover the creek valley and underlie the tailings. Unlike the tailing I, a hardpan level has not been observed in tailing IV, which allowed the oxidation of the remnant wastes of layer TIV-A.

All samples were collected using a Teflon shovel in order to avoid metal contamination, double bagged in sealed low O_2 diffusion plastic bags and transported to the laboratory at 4 °C. Before analysis, samples were air-dried and sieved through a 230 mesh; the fraction <63 μm was used for all determinations and experiments carried out in this work.

Five streamwater samples were collected from the Concordia Creek, in the stretch affected by the mine wastes (ALC 1–4,6), while one sample (ALC-5) was taken from a small tributary, a few meters upstream from its confluence with La Concordia creek (Fig. 1). The streamwater samples were collected in June 2014 when baseflow conditions prevailed, and in April 2016 just at the end of the wet period. Thus, sampling is representative of the extreme hydrological conditions predominating at the site (Fall-winter mean precipitation: 3 mm; spring-summer mean precipitation: 149 mm (Bianchi and Yanez, 1992)).

Field determinations consisted of pH, electrical conductivity (EC), total dissolved solids (TDS), temperature, oxidation reduction potential (ORP), and alkalinity measurements. The pH was measured using a Metrohm 827 portable pH-meter with a combined electrode and integrated NTC temperature sensor for automatic temperature compensation. The ORP was determined with a Combined Pt-ring electrode that contains a Ag/AgCl internal reference electrode. The ORP values were adjusted with respect to hydrogen electrode and expressed as Eh. Electrical conductivity (EC) was measured using a Hach portable conductivity meter, and alkalinity was determined in 100 ml samples by titration using 0.16 N H_2SO_4 and bromocresol green-methyl red as end point indicator (Hach Co).

Immediately after collection, samples were filtered *in situ* through 0.22 μm cellulose acetate membrane filters (Millipore Corp.) and divided into two aliquots. The filtration equipment was repeatedly rinsed with sample water prior to filtration. Aliquots used for major cations and trace elements determination (15 ml) were acidified to pH < 2 with ultrapure HNO_3 (>99.999%, redistilled) and stored in pre-cleaned polyethylene bottles. The

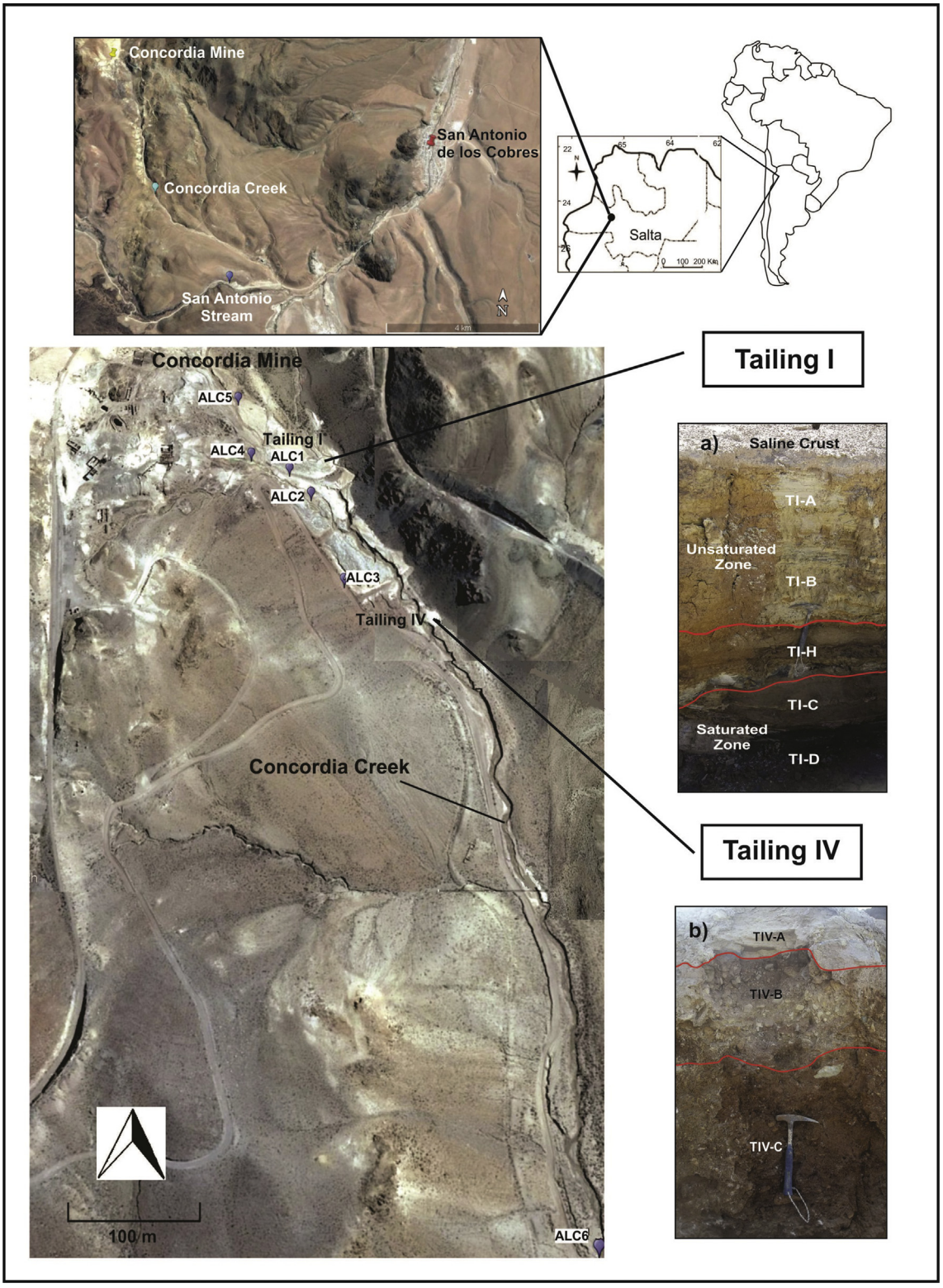

Fig. 1. Map of La Concordia mine site showing the location of water and sediment sampling points; the insets a) and b) show the main sedimentological characteristics of the weathering profiles formed in tailings I and IV respectively.

remaining 20 ml aliquot was stored in polyethylene bottles, without acidifying, at 4 °C for the determination of major anions.

2.3. Acid-generating potential tests

The pH was measured in a paste prepared with ~10 g of sample and 5 ml of MilliQ water, using a Thermo Scientific Orion ROSS® electrode (Pope et al., 2010). This value indicates whether the

sample contains readily available acidity or alkalinity. A paste pH above 7 suggests the presence of reactive carbonate; while a paste pH below 5 suggests that the material contains acidity from prior acid generation.

Static tests are empirical procedures usually conducted to predict the potential of sulphidic wastes to produce acid. The most common static test is the Acid Base Accounting (ABA; Ferguson and Erickson, 1988), which is based on the determination of three main components: 1) acid production; 2) acid consumption; and 3) calculation of net acid production or consumption using 1) and 2) (Lottermoser, 2010).

The ABA test involves a determination of the acid-producing potential and the neutralization capacity of a sample. A common form of expressing the result is to calculate the Net Acid-Producing Potential (NAPP) by simple subtraction of the two chemically determined values:

$$NAPP = MPA - ANC \quad (1)$$

Where MPA is the Maximum Potential Acidity, and ANC is the Acid Neutralization Capacity. If MPA > ANC, the resulting value for NAPP will be positive, thus indicating that the sample will be acid generating; conversely, if MPA < ANC, the NAPP will be negative indicating that the sample should have some acid-neutralizing capacity. Occasionally, the Neutralization Potential Ratio (NPR = ANC/MPA) is used to express the results of the ABA test (Price et al., 1997; Skousen et al., 2002). Values of NPR less than 1 indicate that the sample will eventually lead to acidic conditions (Sherlock et al., 1995), while a ratio greater than 1 is indicative that the sample will not produce acid upon weathering.

The MPA corresponds to the maximum amount of H_2SO_4 produced by sulphidic wastes and can be calculated directly from total sulphur (expressed in wt%) multiplied by 31.25 (to convert to Kg $CaCO_3$ t^{-1}). This calculation assumes that the measured sulphur content occurs as pyrite (FeS_2) which reacts under oxidizing conditions to generate acid, which can then be associated with the mass of $CaCO_3$ required to neutralize the acid through eq. (2):

$$2\ CaCO_3 + H_2SO_4 \rightarrow 2\ Ca^{2+} + 2\ HCO_3^- + SO_4^{2-} \quad (2)$$

The use of the total sulphur to estimate the MPA is a conservative approach because some sulphur may occur in forms other than pyrite. Sulphate-sulphur and native sulphur, for example, are non-acid generating sulphur forms, while some other metal sulphides (e.g. covellite, chalcocite, sphalerite, galena) yield less acidity than pyrite when oxidized. In consequence, in sulphate rich systems, sulphide-sulphur contents should be better used in MPA calculations rather than total S (MEND, 1991).

The ANC was determined following the methodology described in MEND (1991). A known volume of 0.05 M HCl was added to ~2.0 g of dried sample. The suspension was heated to nearly boiling and then, a volume of deionized water was added in order to complete a final volume of 125 ml. The obtained suspension was boiled for 1 min and then cooled to room temperature before being back-titrated with 0.48 M NaOH to pH 7.0. The ANC is reported as kg $CaCO_3$ t^{-1}.

In addition, the Net Acid Generation (NAG) test directly evaluates the generation of sulphuric acid by the accelerated oxidation of sulphides present in the samples. A final NAG pH greater than or equal to 4.5 classifies the sample as non-acid forming. A final NAG pH less than 4.5 confirms that sulphide oxidation generates an excess of acidity and classifies the material as higher risk (Schafer, 2000; Liao et al., 2007).

To perform the NAG test, 250 ml of 15% H_2O_2 was added to ~2.5 g of pulverized sample; the suspension was placed inside a fume hood for 24 h and then boiled for 1 h. After cooling to room temperature, the final pH (NAGpH) was recorded.

2.4. Acid mine-drainage index

The acid mine-drainage index (AMDI) proposed by Gray (1996) was calculated in order to compare the impact of AMD in the study area with other AMD-impacted sites around the world. For calculation, seven parameters (qi) considered as the most indicative of AMD contamination (i.e. low pH, high sulphate and associated cations) and their respective weightings (wi) are used (Table SF-1). Weighting express the relative indicator value of each parameter, estimated by consideration of (a) the concentration of parameters in raw and diluted AMD, (b) their sorption properties, (c) the effect of neutralization on concentration, (d) the relevance of concentration to AMD formation, and (e) detection limits of the analytical procedures used. The AMDI score is calculated using equation (3):

$$AMDI = [\sum (q_i w_i)]^2 / 100 \quad (3)$$

Where $q_i w_i$ are the water quality ratings of the parameter listed in Table SF-1. The AMDI values range from 0 to 100, with values closer to 0 corresponding to raw AMD or to highly contaminated waters (Table SF-2).

2.5. Chemical analysis

2.5.1. Bulk chemical composition and density of sediments

The near-total chemical composition of the tailing's layers was determined in sediment extracts obtained after acid digestion. Briefly, a 0.25 g split is heated in HNO_3-$HClO_4$-HF to fuming and taken to dryness. The residue is dissolved in HCl and solutions are analysed by ICP-OES (Spectro – model Arcos). The accuracy of the results for major, minor, and trace elements was checked against measurement of OREAS25A-4 A and OREAS45E standards, which were carried out along with sample analysis.

Sulphide-sulphur was determined by adding 50 ml of 30% H_2O_2 to ~2 g of the sieved samples; the obtained suspensions were placed inside a fume hood for 24 h and then boiled for 1 h. Then, the suspensions were centrifuged at 5000 rpm for 15 min and then filtered through a 0.22 μm cellulose membrane filter for the analysis of S as SO_4^{2-} by ion chromatography.

The density of sediments accumulated in the study tailings was determined following the pycnometer method based on Blake and Hartge (1986) and Flint and Flint (2002).

2.5.2. Chemical composition of streamwater

Anions (Cl^-, F^-, NO_3^-, and SO_4^{2-}) in streamwater samples were determined by chemically suppressed ion chromatography with conductivity detection (Thermo Scientific™Constametric 3500), while cations and trace elements were measured by ICP-MS (Agilent 7500cx). Deionized water (18 MΩcm MilliQ, Millipore Corp.) was used for all solutions and dilutions. Detection limits were 0.16, 0.15, 0.17 and 0.07 mg L^{-1} for Cl^-, F^-, NO_3^-, and SO_4^{2-} respectively.

For all elemental determinations performed by ICP-MS, calibration curves were run before and after each sample series (8–10 samples including blanks and in-between calibration checks). The calibration solutions covered the range of concentration in the samples and were prepared in ultrapure 2% HNO_3 from certified stock solutions. Sample blanks were run to correct background effects on instrument response. Metal concentrations in samples were calculated using the ChemStation spectrometer software. Detection limits were calculated as three times the instrumental standard deviation obtained after 10 replicates of blank solutions. Detection limit was 10.0, 0.3, 1.0, and 0.5 μg L^{-1} for Fe, Cu, Zn, and

Pb respectively.

2.6. Sequential extractions

The procedure of sequential extractions proposed by Dold (2003) specifically for sulphide mine wastes, was conducted in order to identify metal's associations with the following phases: 1) water soluble; 2) weakly adsorbed elements; 3) Fe (III) oxy-hydroxides (i.e., ferrihydrite; schwertmannite, etc); 4) Fe (III) oxides (goethite, hematite, jarosite, etc); 5) primary sulphides. The details of the procedure are shown in Table SF-3. The metal content that remained in the residual fraction was calculated as: $[metal]_{near-total} - \Sigma[metal]_{steps1-5}$. After each extraction, samples were centrifuged at 4000 rpm for 15 min. The obtained supernatants were filtered using 0.22 μm cellulose membranes and the chemical composition was determined by ICP-OES. Detection limit was 10.0, 2.0, 5.0, and 10.0 $\mu g\,L^{-1}$ for Fe, Cu, Zn, and Pb respectively.

2.7. Batch leaching experiments

Batch experiments were performed in order to evaluate the release of metals throughout time in milliQ water. The experiments were carried out by suspending ~1.0 g of dry sample in 50 mL of milliQ water (pH 6.5) and continuously shaking with a rotator shaker. The suspensions were completely withdrawn after 1, 2, 5, and 10 h and 1, 3, 8, 15, 30, 84, 125, 176, 216, 306,366, 456, 576, and 666 days of the start of the experiments, centrifuged at 5000 rpm for 15 min and then filtered through a 0.22 μm cellulose membrane filter for chemical analysis. The pH of the suspensions at the end of each step was measured before separating the supernatant. In all cases, the final pH dropped to <4.0. After each extraction step, the residue was re-suspended in 50 mL of milliQ water (pH 6.5) and the procedure was repeated until the end of the experiment. Trace elements were analysed in acidified dilutions (1% HNO_3) by ICP-MS. Detection limit was 10.0, 0.3, 1.0, and 0.5 $\mu g\,L^{-1}$ for Fe, Cu, Zn, and Pb respectively.

2.8. X-ray diffraction and SEM/EDS

Minerals in the <63 μm size-fraction of the samples were identified by X-ray diffraction (XRD) and scanning electron microscopy/energy-dispersive X-ray spectroscopy (SEM/EDS) measures. The XRD analysis was performed with a PANalytical X'Pert Pro diffractometer operating at 40 kV and 40 mA using Cu-Kα radiation. The XRD data were obtained for random samples in the 2θ range from 5 to 70° (step size: 0.02; 3 s/step) with a detection limit of 1%. Phase identification was carried out using the X'Pert High Score Plus v3.0e software package by PANalytical.

SEM/EDS analysis was performed with a Carl Zeiss Sigma FE-Scanning Electron Microscope. Samples (gently disaggregated with a pestle and mortar) were mixed with Epofix resin and hardener. The samples were left within a pressure vessel for approximately 12 h before being backfilled with araldite resin, and cured in a drying oven (50 °C, ≥4 h). Once set, the sample was polished and subsequently carbon coated before being measured. In addition, SEM was coupled with focused energy dispersive X-Ray analysis (EDS, AZTec. Oxford) in order to perform the elemental semi-quantification.

3. Results and discussion

3.1. Acid-generating potential

Statics tests (paste pH, ABA and NAG) were conducted in order to define the potential acidity generated by the mine wastes accumulated in tailings I and IV. The obtained results are shown in Table 1.

Paste pH varied between 1.4 and 3.7 in all layers of tailings I and IV, revealing the elevated acidity of the system. In general, paste pHs increase with depth in both tailing profiles.

Due to the high proportion of sulphate minerals identified in the uppermost layers of both tailings (Nieva et al., 2016) calculations using the total S content lead to significantly overestimated MPA values. In order to overcome this, the MPA values shown in Table 1 were calculated on the basis of the sulphide percentages. The obtained results reveal that MPA values increase with depth in tailing I from 12.5 to 96.9 kg $CaCO_3\ t^{-1}$, while in tailing IV these values are markedly lower and vary from 0.9 to 1.6 kg $CaCO_3\ t^{-1}$. The values of the ANC are negative in both tailings (Table 1), which is in accordance with the complete absence of acid-neutralizing minerals such as calcite in the sediments. Negative ANC values, thus determine highly positive values of NAPP (ec. 1).

When the corresponding values in Table 1 are expressed in terms of the amount of generated H_2SO_4 (Kg $H_2SO_4\ t^{-1} = \%S(II)$ x 30.6), the results suggest that the oxidation of sulphides in sediments of tailing I may release from ~32.7 to nearly 171 kg $H_2SO_4\ t^{-1}$. The amount of acidity generated by sulphide oxidation in Tailing IV is much lower and varies from 6 to ~9 kg $H_2SO_4\ t^{-1}$.

The total amount of $CaCO_3$ required to neutralize the H_2SO_4 that could be potentially generated by sulphide oxidation in the studied tailings can be constrained on the basis of the ABA results, the dimensions of each layer in tailings I and IV and their corresponding densities. Table SF-4 summarizes the data used for this calculation and the obtained results reveal that the estimated amount of acidity (expressed in terms of tons of $CaCO_3$) generated by La Concordia wastes is about 375 t just considering the impact of tailings I and IV. Because tailing II and tailing III (not described in this work) have characteristics similar to those of tailing I, it could be reasonably to estimate that the acidity potentially generated by these wastes may account for about 1100 t of $CaCO_3$.

Results of the NAG test are in agreement with those of the ABA test. The pH values recorded at the end of the test (final NAGpH) are lower than 4.5 in all samples (Table 1) indicating that these sediments are acid-producers.

The geochemical classification plot proposed by Smart et al. (2002), combines NAG and NAPP values to evaluate the potential of a sample to generate acid (Figure SF-1). According to this, the studied wastes classify as potentially acid forming (PAF field), indicating that they are likely to generate acidic drainage when exposed to atmospheric conditions.

3.2. Metal concentrations and phase associations

The bulk chemical composition of the layers described in tailings I and IV has been previously reported (Nieva et al., 2016), while the near-total concentration of Fe, Cu, Zn and Pb are reported in Table SF-5. Most elements in tailing TI are enriched in layers TI-B and TI-H (Fig. 2a), while they are markedly depleted in the layer located just beneath the hardpan (TI-C).

Cu and Zn are mainly associated with the soluble fraction. The proportions of these soluble phases are rather constant throughout the profile (Table SF-3) with values that vary from ~62 to 69% and from ~64 to 73% of Cu and Zn, respectively. However, the soluble Cu and Zn phases account for just 21% and 15% of the near-total concentration respectively in the hardpan layer (TI-H), where these two elements remain preferentially associated with the residual fraction (~76 and ~82% of the near total concentrations of Cu and Zn respectively). Acid soluble Cu/Zn hydroxysulfates minerals, commonly associated with sulphidic mine wastes (Hammarstrom et al., 2005) may account for the metal concentrations measured

Table 1
Paste pH and results of acid base accounting (ABA) and NAGpH tests performed in samples of tailings I and IV. (*) Calculated on the basis of S(II) contents.

Sample			ABA					NAG
	Depth	Paste pH	S	S(II)	MPA (*)	ANC	NAPP	NAGpH
	(cm)		(%)	(%)	(Kg $CaCO_3$ t^{-1})			
Tailing I								
TI-A	0–60	1.88	2.1	0.4	12.5	−20.4	32.9	2.2
TI-B	60–80	1.49	5.1	0.4	12.5	−24.8	37.3	2.3
TI-H	80–90	1.40	5.8	2.0	62.5	−104.2	166.7	2.1
TI-C	90–116	2.02	1.6	1.6	50.0	−63.6	113.6	2.6
TI-D	116–189	2.34	3.1	3.1	96.9	−76.3	173.1	2.4
Tailing IV								
TIV-A	0–60	2.47	0.8	0.05	1.6	−5.94	7.5	2.6
TIV-B	60–105	2.98	1.6	0.05	1.6	−4.62	6.2	2.9
TIV-C	105–205	3.68	0.7	0.03	0.9	−8.34	9.3	2.6

in this fraction. In the remaining layers, the residual Cu/Zn phases are the next more important after the water soluble fraction.

The associations of Fe with the extracted fractions are slightly different to the ones described for Cu and Zn. The proportion of Fe associated with the water-soluble fraction is not dominant as in the case of Cu and Zn, but still important. The concentrations of the water-soluble Fe phases are likely derived from the dissolution of the highly soluble salts rozenite and melanterite, already identified by XRD in the uppermost layers of tailing I (Nieva et al., 2016). Although the proportion of the soluble fraction slightly decreases with depth, the highest accumulation of Fe-soluble phases occurs at ~60 cm depth, in the layer TI-B. This is likely associated with the mechanisms that control the precipitation of salts by evaporation in the study area. Bea et al. (2010) have modeled this process in tailings accumulated in an arid region of Chile and suggest that the low relative humidity during the summer causes evaporation, making water flow upwards. Solute concentrations in the upflowing water are dramatically increased, triggering the precipitation of salts and the formation of efflorescent crusts. Progressive evaporation leads to reduced pore-water content and thus prevents upward fluxes. Therefore, the evaporation front is slightly displaced downwards, where efflorescences continue to grow within the pore volume.

The presence of amorphous and crystalline Fe (hydr)oxides and Fe(III) hydroxysulfates throughout the profile determines the elevated proportions of Fe associated with the oxidizing fractions (Fig. 2a; Table SF-5). These amorphous and crystalline oxides are common products of the pyrite oxidation (e.g., Lottermoser, 2010). Finally, a minor proportion of Fe is associated with primary sulphides identified by SEM/EDS as sub-euhedral crystals of pyrite and arsenian pyrite throughout the profile and with silicates such as biotite and amphiboles derived from the weathering of the dacite dome, one of the host rocks of the mineralized vein.

Unlike Cu, Zn and Fe, bulk Pb concentrations show little variation in the tailing I sequence, with the exception of layers TI-A and TI-C where this element is moderately depleted (Fig. 2a). Lead occurs mostly as a weakly adsorbed species along the weathering profile, except in layer TI-B where residual Pb dominates (Table SF-3). This in consonance with a number of XAFS studies of Pb^{2+} in mine wastes that have found clear evidence for significant Pb^{2+} adsorption onto Fe and Mn (hydr)oxides as well as on humic materials (e.g., Hesterberg et al., 1997; O'Day et al., 1998, 2000). Pb-bearing salts, such as anglesite (Fig. 3a) are sparingly soluble in water and therefore, the association of this element with the soluble fraction is low and nearly constant throughout the profile (~6% of the near total Pb concentration, Table SF-3). The proportion of Pb associated with primary sulfides increases in depth, where crystals of galena have been frequently observed (Fig. 3b). The high proportion of Pb in the residual fraction is in agreement with the limited mobility of this element and its capacity of being included as an impurity within the structure of silicates such as zircon (Watson et al., 1997) and feldspars (Cherniak, 1995).

The profile sampled in tailing IV shows the transition between the mine waste sediments accumulated at the bottom of the dam and the coarse sands and conglomerates of the Pirgua subgroup that underlies the tailing's dams. Therefore, metal concentrations and solid speciation across this profile may reveal the dispersion of metals that result from the interaction between infiltrating water and the basal sediments of the site.

The near-total concentrations of Cu, Zn and Pb in the tailing IV profile are about one order of magnitude lower than the corresponding concentrations determined in tailing I, whereas the Fe near-total concentrations are in the same range in both tailings (Fig. 2b). Lower metal concentrations in layer TIV-A than those measured in tailing I indicate that wastes in tailing IV have been more intensively leached out. The in-depth distribution of bulk metal concentrations and the solid associations shown in Fig. 2b suggest that metals released to the infiltrating water as a consequence of the alteration of the mine wastes in layer TIV-A are likely transported downward in solution and retained in the sediments of the Pirgua subgroup by precipitation and/or adsorption onto clay minerals or Fe (hydr)oxides.

Although the proportion of soluble Cu and Zn phases are important throughout profile IV, they are not dominant as in the case of tailing I (Fig. 2b, Table SF-5). Soluble salts of Cu and Zn have been observed by SEM/EDS and consist mostly of Cu and Zn sulfates. Interestingly, these soluble salts accumulate in the bottom layer TIV-C, located just above the water table level. On the other hand, Cu seems to be highly scavenged by clays and amorphous and crystalline Fe oxides, particularly in the finest grain-sized sediments of the Pirgua subgroup (layer TIV-B) while the proportion of Zn associated with these phases is less important across the profile. A dominant proportion of Zn is associated with the reducible fraction in layer TIV-A, which suggests that Zn sulphides are in some extent more resistant to weathering than Cu sulphides. Finally, the proportions of Cu and Zn associated with the residual fraction could be assigned to acid soluble hydroxysulfates and some other resistant minerals present in the regional rocks.

A major proportion of Fe remains associated with the residual fraction in tailing IV and therefore, it is mostly present in the rock-forming minerals of the dacite dome such as biotite, hornblende and pyroxenes. The next more abundant Fe phase corresponds to amorphous and crystalline (hydr)oxides that are frequently found in the form of red coatings covering the tailings walls and precipitated onto mineral surfaces or rock fragments (inset, Fig. 1). Plumbojarosite ($PbFe_3(SO_4)_4(OH)_{12}$) that has already been identified in all layers in tailing IV (Nieva et al., 2016) also accounts for Fe

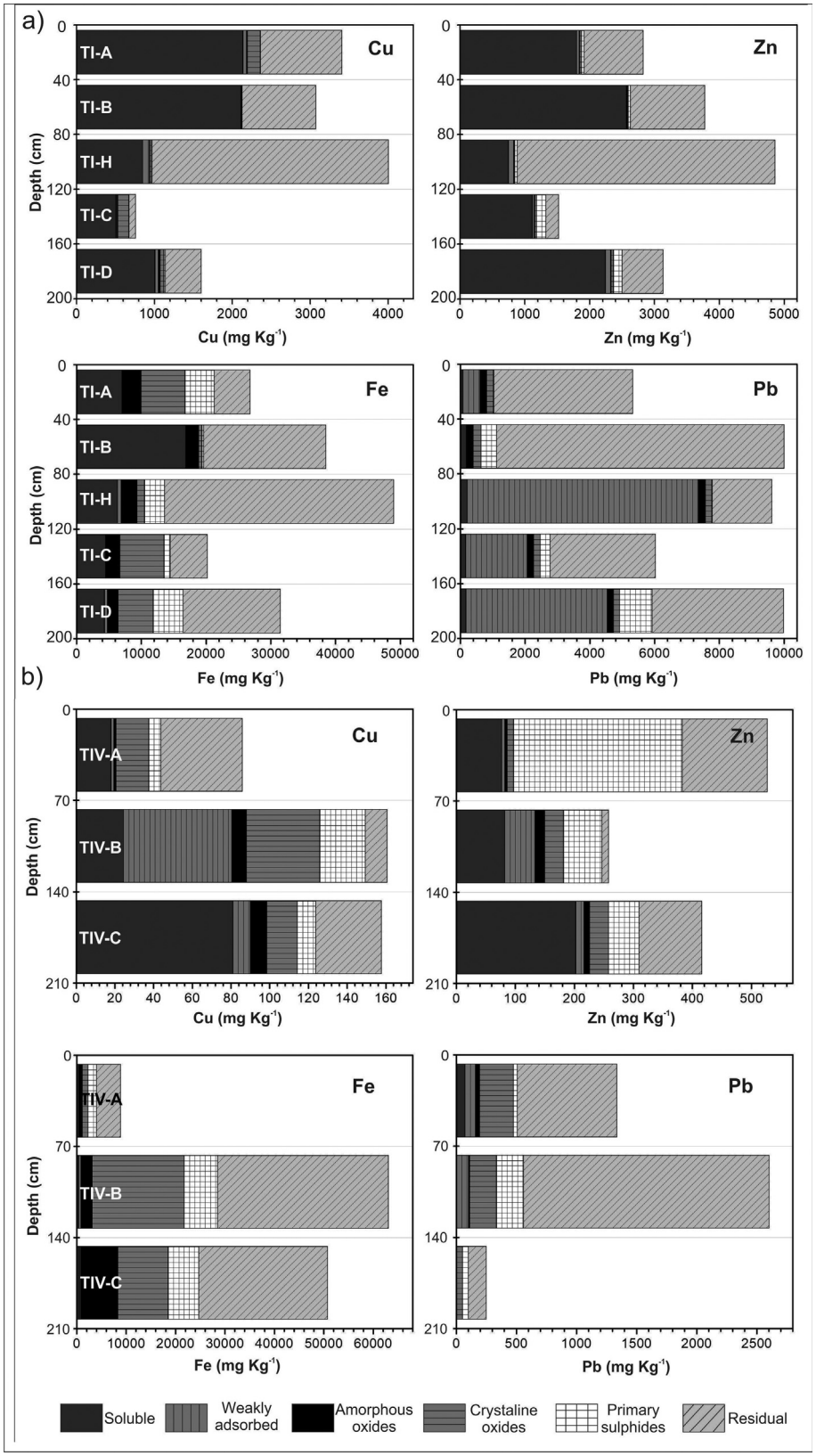

Fig. 2. Distribution of the near total Cu, Zn, Fe and Pb concentrations and phase associations determined in the sequential extraction experiments along the profile of a) tailing I and b) tailing IV.

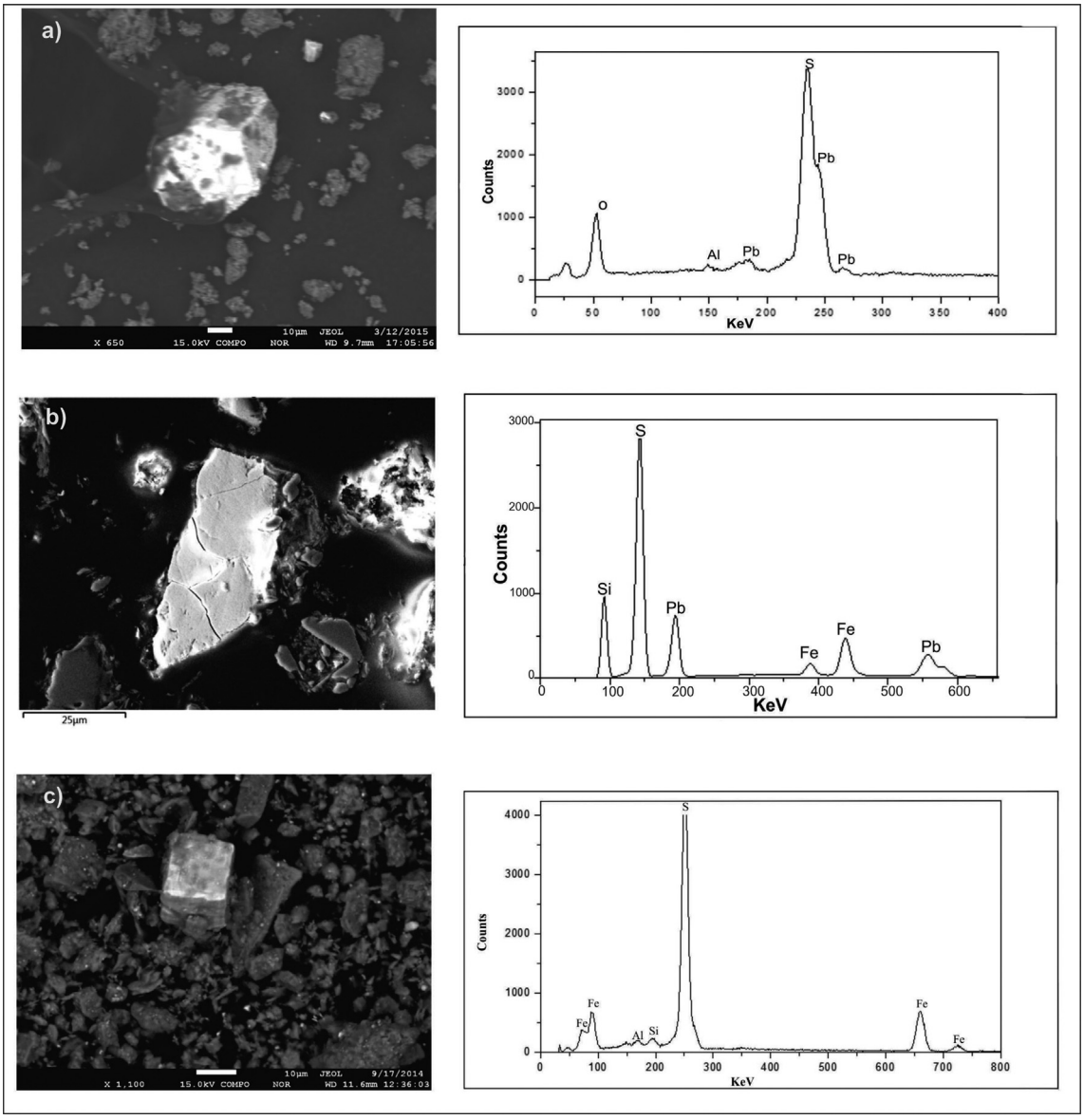

Fig. 3. SEM images and EDS spectra of some minerals identified in tailings sediments. a) subhedral crystal of anglesite; b) anhedral crystals of galena; c) cubic crystal of pyrite.

associated with this fraction. Euhedral cubic crystals of pyrite (Fig. 3c) frequently observed in these sediments account for the proportion of Fe associated with primary sulphides indicated in Fig. 2b. Finally, the proportion of Fe associated with soluble Fe salts is the least abundant and it increases with depth.

The proportion of water soluble Pb accounts for ~5% of the near-total Pb concentration in the uppermost layer of tailing IV, while it is nearly negligible in the bottom layers (Table SF-5). This suggests that Pb released after the oxidation of galena and/or some other polymetallic sulphides in layer TIV-A is rapidly scavenged by adsorption onto Fe (hydr)oxides during the downward movement of water. Another important proportion of Pb is associated with the residual fraction indicating that this element is present as an impurity in the regional rock-forming minerals.

3.3. Release of metals with time

Figs. 4 and 5 illustrate the results obtained in leaching experiments performed with the suspensions of the studied sediments. The release of all elements show a general trend characterized by a rapid increase in all aqueous concentrations during the first hour of sediment-water interaction followed by a decline in the release rates thereafter.

The accumulated metal concentrations released after >600 days of sediment-water interaction from mine wastes of tailing I were the highest in suspensions of the layer TI-B, while the lowest values corresponded to those registered in suspensions of TI-C for all metals except Pb. Among the analysed elements, Cu, Zn, and Fe are the more readily mobile as more than 60% of their near-total concentrations was released until the end of the experiments. Conversely, the proportion of Pb released to water was the lowest, typically <10% of its near-total content, but it may reach values as high as 25–48% in layers TI-B and TI-D respectively. The absolute concentrations of Fe released during the experiments were the highest in all layers.

The concentrations of metals released from mine wastes and sediments of the tailing profile IV after >600 days of sediment-water interaction were remarkably lower than those measured in

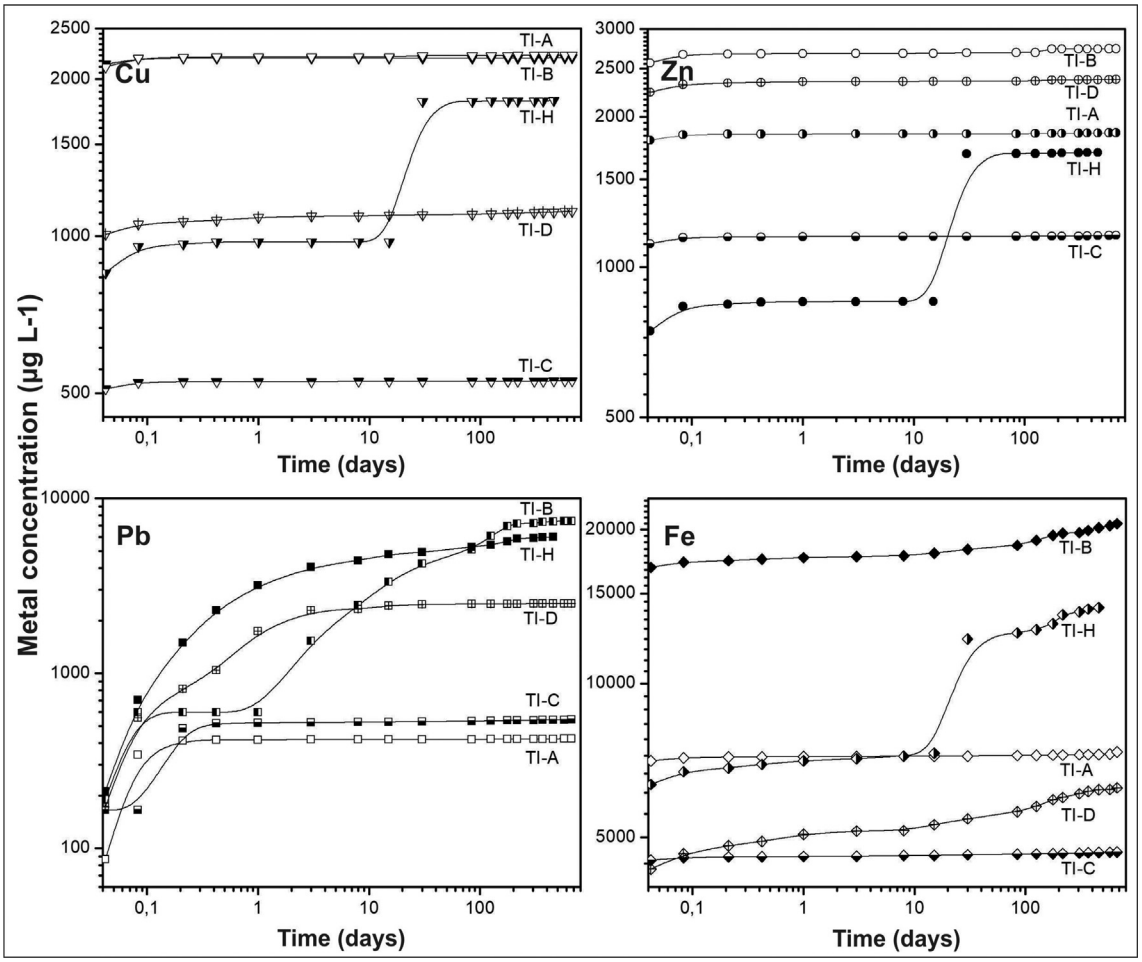

Fig. 4. Cumulative release of Cu, Pb, Zn and Fe with time measured in suspensions of sediments sampled from tailing I in MilliQ water. Note that log scale is used for both axes. The curves drawn through the measured points are indicative only of the general trend followed by the samples. %RSD: 1.97 (Pb); 0.77 (Fe); 2.41 (Cu); 2.03 (Zn). White circles: Zn; black circles: Pb; white triangles: Cu; black triangles: Fe.

wastes of tailing I. Among the analysed metals, Cu and Zn were released in elevated proportions from all layers, while the highest Pb concentrations were released from layer TIV-A (~70% of the corresponding near-total concentration). The proportion of Fe released from the two uppermost layers was ~1.5%, while it reached 28% of the respective near-total content in the bottom layer.

The general trend of release described above shows particular features among the analysed elements. Cu and Zn follow a similar trend in most layers of the studied tailing profiles. As seen in Figs. 4 and 5, a rapid increment in the aqueous concentrations of these elements occurs in the first 3 h of sediment-water interaction and then, equilibrium conditions are reached, suggesting that these elements are contributed from the rapid dissolution of the Cu- and Zn- bearing (hydrous)sulfates disseminated within the sediment's matrix. The release of these elements in layers TI-H and all layers of tailing IV also follows this trend until 10–15 days of sediment-water reaction when new contributions from less soluble phases occur. A longer exposure to water probably enhances some other mechanisms of release, such as desorption or dissolution of less the soluble hydroxysulfates.

The salts of Pb are sparingly soluble and thus, the elevated concentrations of this element released in the first hour of sediment-water interaction should be likely due to contributions from desorption rather than form dissolution of Pb-bearing minerals. This phase seems to be the unique contribution to the pool of aqueous Pb concentrations in all layers of tailing I, except layer TI-B. In this layer and in all layers of tailing IV, increasing Pb concentrations are observed after 5 h and ~3 days of leaching. During this second stage, the rates of release become slower, likely representing the dissolution of less soluble Pb salts. Equilibrium conditions are reached after 10–30 days, except in layers TI-B and TIV-B where Pb concentrations still increase until the end of the experiment.

With the exceptions of layers TI-H, TI-D and all layers in tailing IV, the release of Fe occurs in the first hour of water-sediment contact, and likely corresponds to the dissolution of the highly soluble (hydrous)sulphates rozenite and melanterite disseminated within the wastes. No other contributions of Fe were observed until the end of the experiment. In TI-H, TI-D and TIV-A, contributions of Fe from less soluble phases are observed after ~15 days of leaching. These contributions could be mostly associated with the dissolution of jarosite, szomolnokite or amorphous Fe (hydr)oxides minerals. Finally, low contributions of Fe are detected after ~100 days of leaching in these layers and in layers TIV-B and TIV-C that may likely represent the release of dissolved Fe by sulphides oxidation or by the hydrolysis of Fe-bearing silicates.

The observed trends suggest that when mine wastes interact with water in an oxidizing environment, a near immediate (less than 1 h) release of metals associated with readily soluble salts occur, thus producing a rapid increment in the metal concentrations of the infiltrating water. A longer exposure to water seems to

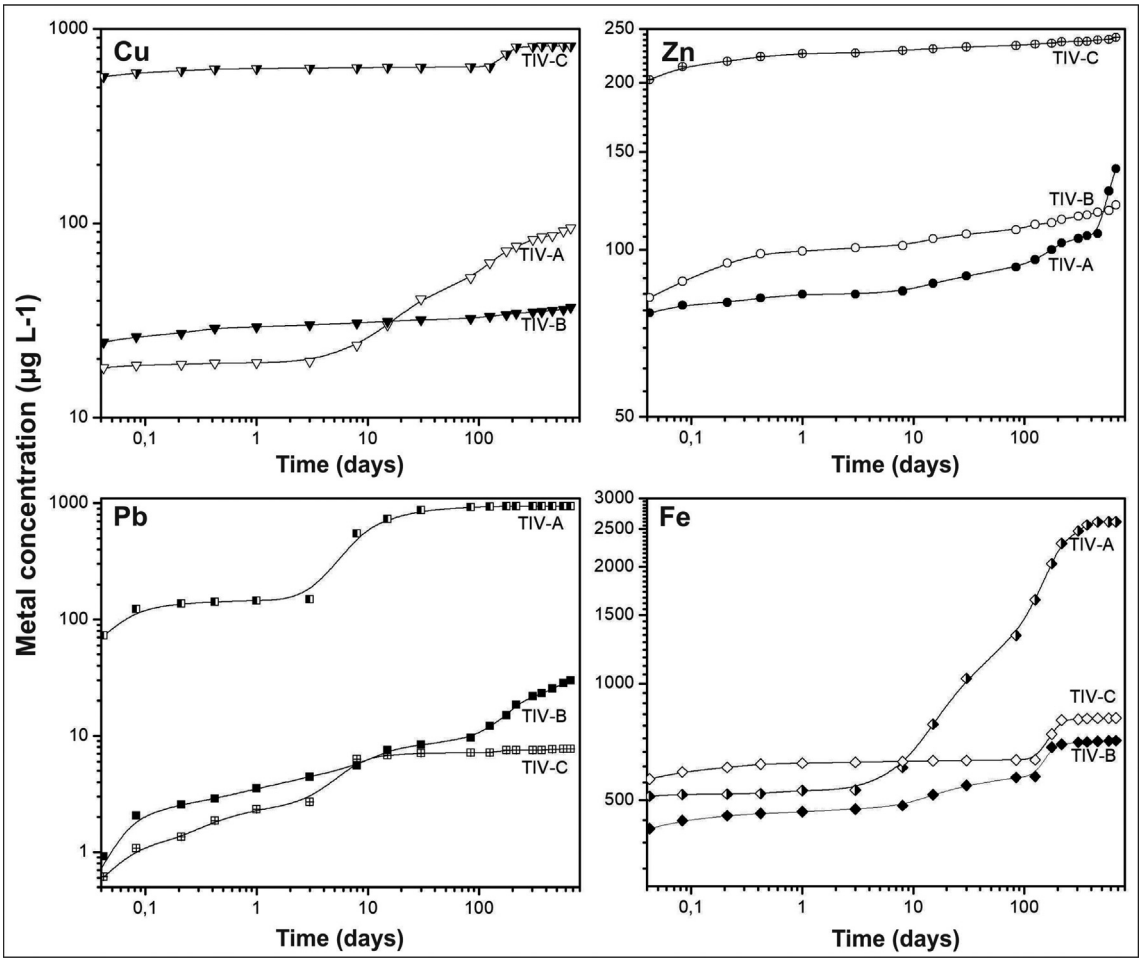

Fig. 5. Cumulative release of Cu, Pb, Zn and Fe with time measured in suspensions of sediments sampled from tailing IV in MilliQ water. Note that log scale is used for both axes. The curves drawn through the measured points are indicative only of the general trend followed by the samples. %RSD: 1.97 (Pb); 0.77 (Fe); 2.41 (Cu); 2.03 (Zn). White circles: Zn; black circles: Pb; white triangles: Cu; black triangles: Fe.

enhance the release of metals from less mobile phases, likely by desorption from Fe (hydr)oxides sites and/or by dissolution of less soluble phases such as metal hydroxysulfates. In exposure times longer than ~120 days, low increments in metal concentrations with time are likely due to contributions from oxidation of the remnant metal sulphide grains and/or the hydrolysis of silicate minerals.

3.4. Acidity and metal concentrations in the La Concordia stream

The weathering of the studied mine wastes has a direct impact on the physico-chemical characteristics of the La Concordia creek, as revealed by the parameters determined in the stream water samples collected along the affected stretch, and shown in Table 2.

Low pH values prevail in the stretch affected by the mine wastes with values that ranged between 3.15 and 3.70. This acidic range of pH values remains nearly constant in the studied ~1 km length stretch in both periods of sampling. The electrical conductivity (EC) is elevated and also remains nearly constant in the flow direction. The EC values are controlled by the hydrological conditions in the basin, as the average values were slightly lower at the end of the humid period (1.84 ± 0.2 mS cm^{-1}) than those measured under baseflow conditions (2.25 ± 0.1 mS cm^{-1}). Similarly, redox conditions were slightly more oxidizing in April 2016 than in June 2014.

The relative concentration of major cations along the analysed stretch was $Na^+ > Mg^{2+} > Ca^{2+} > K^+$, while SO_4^{2-} is the dominant anion in the entire section. In general, solute concentrations were more diluted at the end of the wet period (April 2016).

The acid mine drainage index (AMDI) values calculated for La Concordia water samples are reported in Table 3a. Final scores reveal that, under baseflow conditions, water quality is highly impacted by direct contributions of AMD with little or no dilution in the stretch located immediately downstream the mine adit and adjacent to tailing I. Only the sample collected ~75 m upstream the mine adit discharge (ALC-5) shows a higher score, likely because it is not directly impacted by the wastes leachates. The AMDI values calculated for the humid period (Table 3b) are slightly higher than those in the dry season, thus revealing the dilution effect due to increased runoff and groundwater discharge. Whatever the hydrological period, the scores determined in La Concordia creek are low when compared with the scores calculated in other impacted mine sites in the world (e.g., Soltani et al., 2013) and reveal the low capacity for natural attenuation of the system.

Although the waters of the Concordia stream are not used directly for drinking water supply, this stream flows into the San Antonio River, whose waters constitute the main source of water supply for the town of San Antonio de los Cobres. Therefore, metal concentrations are referred to national and international guideline values for drinking waters. As seen in Table 2, metal concentrations exceed the recommended guideline value for drinking waters set

Table 2
Chemical composition of water samples collected in the impacted stretch of La Concordia creek on a) June 2014 and b) April 2016. bdl: below detection limit; nd: not determined.

a)

Sample	pH	Conductivity	Eh	Na^+	K^+	Mg^{2+}	Ca^{2+}	Cl^-	SO_4^{2-}	HCO_3^-	Fe	Pb	Cu	Zn
		mS cm^{-1}	mV	mgL^{-1}										
ALC1	3.21	2.42	353	43.1	15.4	43.0	40.3	21.1	1258.5	bdl	235.9	1.58	1.21	28.7
ALC2	3.56	2.35	385	45.6	14.1	47.9	43.1	26.9	1728.6	bdl	245.8	1.34	1.43	32.03
ALC3	3.66	2.18	410	36.8	5.7	38.6	34.8	23.2	1311.9	bdl	72.68	0.62	3.79	28.41
ALC4	3.25	2.32	311	38.7	14.4	38.7	35.1	26.4	1525.7	bdl	219.7	1.44	1.16	27.3
ALC5	3.21	nd	nd	28.9	4.9	21.0	19.4	17.6	706.6	bdl	7.71	0.25	1.85	15.83
ALC6	3.18	1.98	456	38.0	5.3	43.3	39.7	26.9	1634.8	bdl	17.33	0.08	3.85	27.85

b)

Sample	pH	Conductivity	Eh	Na^+	K^+	Mg^{2+}	Ca^{2+}	Cl^-	SO_4^{2-}	HCO_3^-	Fe	Pb	Cu	Zn
		mS cm^{-1}	mV	mgL^{-1}										
ALC1	3.70	1.70	436	26.47	5.64	21.24	9.71	31.07	1005.49	bdl	32.05	0.75	3.96	13.92
ALC2	3.30	1.97	382	23.42	8.47	21.98	11.03	17.95	845.18	bdl	99.25	0.55	0.42	11.77
ALC3	3.42	1.95	406	19.62	4.11	19.78	10.26	23.20	1111.22	bdl	28.06	0.15	1.65	12.68
ALC4	3.45	1.94	355	35.33	13.78	33.39	16.81	23.70	1169.20	bdl	158.25	0.80	0.59	17.71
ALC5	3.15	1.55	542	30.61	3.05	23.84	9.99	16.79	675.18	bdl	5.38	0.05	1.83	17.14
ALC6	3.29	1.98	445	41.03	8.65	41.24	19.76	38.74	1354.96	bdl	25.17	0.16	3.44	25.15

Table 3
Acid mine-drainage index (AMDI) in water samples collected in the impacted stretch of La Concordia creek on a) June 2014 and b) April 2016.

a)

Parameter	Weighting	ALC1	ALC2	ALC3	ALC4	ALC5	ALC6
	(wi)	June					
pH	0.2	8	10	10	8	8	8
SO4 (mg/l)	0.25	6	4	6	5	15	4
Fe (mg/l)	0.15	6	6	9	6	12	11
Al (mg/l)	0.1	7	7	7	7	7	6
Zn (mg/l)	0.12	6	6	6	6	7	6
Cd (μg/l)	0.1	5	6	6	6	6	6
Cu (mg/l)	0.08	6	6	6	6	6	6
Σ (qiwi score)		44	45	50	44	61	47
Final Score		19.3	20.2	25.0	19.3	37.2	22.1

b)

Parameter	Weighting	ALC1	ALC2	ALC3	ALC4	ALC5	ALC6
	(wi)	April					
pH	0.2	11	9	9	9	8	8
SO4 (mg/l)	0.25	13	14	7	7	15	6
Fe (mg/l)	0.15	10	9	10	7	12	10
Al (mg/l)	0.1	6	9	7	8	6	6
Zn (mg/l)	0.12	7	7	7	7	7	6
Cd (μg/l)	0.1	6	7	7	7	7	6
Cu (mg/l)	0.08	9	10	6	7	6	6
Σ (qiwi score)		62	65	46	52	61	48
Final Score		38.4	42.25	21.2	27.04	37.2	23.0

by the Argentinean and international regulations (i.e., Código Alimentario Argentino, CAA, 2007; WHO, 2004) in both sampling periods. Dissolved Fe concentrations are from one to three orders of magnitude higher than the CAA guideline value (0.3 mg L^{-1}) and they show a general trend of decreasing concentrations downstream. Even though Fe concentrations at the end of the wet period are much lower, they still exceed the guideline requirements for drinking water.

Lead concentrations are up to 30 times higher than the recommended guideline value (0.05 mg L^{-1}). Like iron, concentrations of Pb decrease in the flow direction and also in the wet season, but they are never below the drinking water requirements. The concentrations of Cu exceed the corresponding CAA guideline value for drinking water (1.0 mg L^{-1}) along the analysed stretch during the dry period, while in the wet season some concentrations meet the CAA requirements. During the dry season, Cu concentrations are high and rather constant along the stretch, while at the end of the wet season, concentrations are spatially variable. Similarly, Zn concentrations are from twice to nearly six times higher than the recommended maximum concentration for drinking water (5.0 mg L^{-1}). The measured contents are higher during the dry period than at the end of the wet season but the spatial variability of concentrations is limited in both periods.

4. Conclusions

After more than three decades of exposure to surficial conditions, mine wastes accumulated in tailing dams in the La Concordia mine have been strongly weathered. The oxidation of primary sulphides, mainly pyrite and arsenopyrite, led to the formation of Fe (hydrous)sulphates, Fe/Al hydroxysulphates as well as Fe (hydr) oxides that precipitated in the form of crusts at the tailings' surface, as disseminated salts in the uppermost layers of the tailings, or as red coatings covering the exposed tailings' walls. In addition, a highly acid drainage rich in Fe, Cu, Pb and Zn is generated during such process and leaks into La Concordia, the small creek that crosses the site. As a consequence, the water quality is affected, having low pH values (i.e., pH < 4) and concentrations of metals that exceed the guidelines values for drinking water. Metal concentrations are slightly lower during the wet season (April) than during the dry season (June), but concentrations are not significantly different likely because annual rainfall is too low to produce important dilution in ionic concentrations. Although AMDI values reveal a slight improvement in the water quality during the wet season, the scores are still very low when compared with some other mine impacted sites around the world revealing the low capacity for natural attenuation of the system.

The acid generating potential tests performed with wastes accumulated in the tailing dams of La Concordia mine indicate that about 1100 t of $CaCO_3$ are required to neutralize the acidity generated by sulphide oxidation in the site. In addition, these wastes have the potential of releasing elevated concentrations of heavy metals to la Concordia Creek. The more labile fraction is composed of highly soluble efflorescence salts formed by the intense evaporation that dominates in this arid and high altitude region. These

salts consist of Fe and Mg (hydrous)sulphates and they play an important role in the control of metal mobility, as they rapidly dissolve in contact with water releasing Fe, but also Cu and Zn usually scavenged by such minerals. These salts form salt crusts that cover the entire site, but also precipitate deeper into the pores of the sediment after progressive evaporation cycles. Another important proportion of the analysed metals, particularly Pb, is adsorbed onto Fe (hydr)oxides, thus representing a hazardous reservoir with the potential of mobilizing metals into porewaters and streamwaters with changes in pH and redox conditions. The increment in metal concentrations after exposure of wastes to water for nearly two years, reveal that an important proportion of metals associated with less labile phases can be released to water more slowly and therefore, must be considered as a long term source of heavy metal pollution.

The prevalence of the hardpan layer in three of the four tailings dams at the La Concordia site has prevented bottom sediment from oxidizing and, therefore, the more labile phases of heavy metals have remained accumulated in the layers immediately above the hardpan. On the contrary, in tailing IV, the lack of the hardpan layer promoted the complete oxidation and the partial removal of the mine wastes by erosion allowing the infiltration of metal-rich solutions towards the riverbed sediments, where heavy metals mainly precipitate in the form of highly soluble salts or remain attached to Fe or Mn (hydr)oxides.

The Puna is an environmental fragile region with valuable economic resources and of great ecological importance in the world. Thus, the metal sulphide mine wastes abandoned without a proper treatment in a number of small prospects across this large region of South America, represent hazardous sources of metals and acidity that require urgent remediation practices.

Acknowledgements

Authors wish to acknowledge the assistance of CONICET (PIP Nº 11220150100484CO), ANPCyT (FONCyT, PICT 2015-0313), and UNC (SECyT-UNC 05/I754) whose support facilities and funds were used in this investigation. N.E. Nieva acknowledges a doctoral fellowship from CONICET. L. Borgnino and M.G. Garcia are members of CICyT in CONICET, the National Science Foundation of Argentina. Thanks to Andrea Lojo for the ICP-MS analysis and assistance during laboratory work. We are especially grateful to two anonymous reviewers for suggesting significant improvements to this manuscript.

Appendix A. Supplementary data

Supplementary data related to this article can be found at https://doi.org/10.1016/j.envpol.2018.06.067.

References

Alonso, R.N., 2000. El terciario de la Puna en tiempos de ingresión marina paranense. Rev. Asoc. Geol. Argent. 14, 163–180.
Bea, S.A., Ayora, C., Carrera, J., Saaltink, M.W., Dold, B., 2010. Geochemical and environmental controls on the genesis of soluble efflorescent salts in Coastal Mine Tailings Deposits: a discussion based on reactive transport modeling. J. Contam. Hydrol. 111, 65–82.
Bianchi, D., Yanez, A., 1992. Las precipitaciones en el NOA Argentino, Segunda Edición. INTA Salta.
Blake, G.R., Hartge, K.H., 1986. Bulk density. In: Klute, A. (Ed.), Methods of Soil Analysis. Part 1, second ed., pp. 363–375 Agron. Monogr. 9. ASA and SSSA, Madison, Wisconsin, USA.
CAA Código Alimentario Argentino, 2007. Capitulo XII. Bebidas Hídricas, Agua Y Agua Gasificada. Artículo 982. Res Conj. SPRyRS Y SAGPyA N° 68/2007 Y N° 196/2007. Ley 18284. Marzocchi, Buenos Aires.
Cherniak, D.J., 1995. Diffusion of lead in plagioclase and K-feldspar: an investigation using ruther ford backscattering and resonant nuclear reaction analysis. Contrib. Mineral. Petrol. 120, 358–371.
Chiavazza, H., Prieto, C., 2008. Arqueología de la minería en el sitio precordillerano los hornillos (Reserva Natural Villavicencio -rnv-, Mendoza), 2da ed. Revista de Arqueología Histórica Argentina y Latinoamericana, pp. 45–77.
Descostes, M., Vitorge, P., Beaucaire, C., 2004. Pyrite dissolution in acidic media. Geochem. Cosmochim. Acta 68, 4559–4569.
Dold, B., 2003. Speciation of the most soluble phases in a sequential extraction procedure adapted for geochemical studies of copper sulfide mine waste. J. Geochem. Explor. 80, 55–68.
Druschel, G., Borda, M., 2006. Comment on "Pyrite dissolution in acidic media" by Descostes M, Vitorge P, beaucaire C. Geochem. Cosmochim. Acta 70, 5246–5250.
Ferguson, K.D., Erickson, P.M., 1988. Pre-mine prediction of acid mine drainage. In: Salomons, W., Forstner, U. (Eds.), Dredged Material and Mine Tailings. Springer, Berlin.
Flint, A.L., Flint, L.E., 2002. Porosity. In: Dane, J.H., Topp, G.C. (Eds.), Methods of Soil Analysis. Physical Methods. American Society of Agronomy; Soil Sci Soc of America, Madison, pp. 241–254.
Gray, N.F., 1996. The use of objective index for the assessment of the contamination of surface water and groundwater by acid mine drainage. J Chart Inst Water E 10, 332–341.
Hammarstrom, J.M., Seal, R.R., Meier, A.L., Kornfeld, J.M., 2005. Secondary sulfate minerals associated with acid drainage in the eastern US: recycling of metals and acidity in surficial environments. Chem. Geol. 215, 407–431.
Hedenquist, J.W., Lowenstern, J.B., 1994. The role of magmas in the formation of hydrothermal ore deposits. Nature 370, 519–527.
Hesterberg, D., Sayers, D.E., Zhou, W., Plummer, G.M., Robarge, W.P., 1997. X-ray absorption spectroscopy of lead and zinc speciation in a contaminated groundwater aquifer. Environ. Sci. Technol. 31, 2840–2846.
Idaszkin, Y.L., Carol, E., Alvarez M del, P., 2017. Mechanism of removal and retention of heavy metals from the acid mine drainage to coastal wetland in the Patagonian marsh. Chemosphere 183, 361–370.
Kirschbaum, A., Murray, J., Arnosio, M., Tonda, R., Cacciabue, L., 2012. Pasivos ambientales mineros en el noroeste de Argentina: aspectos mineralógicos, geoquímicos y consecuencias ambientales. Rev. Mex. Ciencias Geol. 29, 248–264.
Lecomte, K.L., Maza, S.N., Collo, G., Sarmiento, A.M., Depetris, P.J., 2017. Geochemical behavior of an acid drainage system: the case of the Amarillo River, Famatina (La Rioja, Argentina). Environ. Sci. Pollut. Res. 24, 1630–1647.
Liao, B., Huang, L.N., Ye, Z.H., Lan, C.Y., Shu, W.S., 2007. Cut-off net acid generation pH in predicting acid-forming potential in mine spoils. J. Environ. Qual. 36, 887–891.
Lottermoser, B.G., 2010. Mine Wastes: Characterization, Treatment and Environmental Impacts, third ed. Springer, Berlin, Heidelberg.
Matteini, M., Mazzuoli, R., Omarini, R., Cas, R., Maas, R., 2002. The geochemical variations of the upper Cenozoic volcanism along the Calama-Olacapato-El Toro trasnversal fault system in central Andes (24°S): petrogenetic and geodynamic implications. Tectonophysics 345, 211–227.
MEND, 1991. Acid Rock Drainage Prediction Manual. MEND Project 1.16.1b, Report by Coastech Research. MEND. Natural Resources Canada.
Murray, J., Kirschbaum, A., Dold, B., Guimaraes, M., Pannunzio Miner, E., 2014. Jarosite versus soluble iron-sulfate formation and their role in acid mine drainage formation at the Pan de Azúcar mine tailings (Zn-Pb-Ag), NW Argentina. Minerals 4, 477–502.
Nieva, N., Borgnino, L., Locati, F., García, M.G., 2016. Mineralogical control on arsenic release during sediment–water interaction in abandoned mine wastes from the Argentina Puna. Sci. Total Environ. 550, 1141–1151.
Oblasser, A., Chaparro, E., 2008. Estudio comparativo de la gestión de los pasivos ambientales mineros en Bolivia, Chile, Perú y Estados Unidos. CEPAL, serie Recursos Naturales e Infraestructura, p. 84. United Nations.
O'Day, P.A., Carroll, S.A., Waychunas, G.A., 1998. Rock-water interactions controlling zinc, cadmium, and lead concentrations in surface waters and sediments, U.S. Tri-State Mining District. I. Molecular identification using X-ray absorption spectroscopy. Environ. Sci. Technol. 32, 943–955.
O'Day, P.A., Carroll, S.A., Randall, A., Martinelli, R.E., Anderson, S.L., Jelinski, J., Knezovich, J.P., 2000. Metal speciation and bioavailability in contaminated estuary sediments, Alameda Naval Air Station, California. Environ. Sci. Technol. 34, 3665–3673.
Oyarzun, R., Márquez, A., Lillo, J., López, I., Rivera, S., 2000. Reply to Discussion on "Giant versus small porphyry copper deposits of Cenozoic age in northern Chile: adakitic versus normal calc-alkaline magmatism. Miner. Deposita 36, 794–798.
Pope, J., Weber, P., Mackenzie, A., Newman, N., Rait, R., 2010. Correlation of acid base accounting characteristics with the Geology of commonly mined coal measures, West Coast and Southland, New Zealand. Zeal. J. Geol. Geophy 53, 153–166.
Price, W.A., Morin, K., Hutt, N., 1997. Guidelines for the prediction of acid rock drainage Part II. Recommended procedures for static and kinetic testing. In: Proceedings from the 4th International Conference on Acid Rock Drainage, vol. 1, pp. 15–30.
Riller, U., Petrinovic, I.A., Ramelow, J., Greskowiak, J., Strecker, M., Oncken, O., 2001. Late Cenozoic tectonism, caldera and plateau formation in the central Andes. Earth Planet Sci. Lett. 188, 299–311.
Schafer, W.M., 2000. Use of the net acid generation pH test for assessing risk of acid generation. In: Proceedings from the 5th International Conference on Acid Rock Drainage, ICARD, 1, pp. 613–618.
Sherlock, E.J., Lawrence, R.W., Poulin, R., 1995. On the neutralization of acid rock drainage by carbonate and silicate minerals. Environ. Geol. 25, 43–54.

Skousen, J., Simmons, J., McDonald, L.M., Ziemkiewicz, P., 2002. Acid-base accounting to predict post-mining drainage quality on surface mines. J. Environ. Qual. 31, 2034–2044.
Smart, R., Skinner, B., Levay, G., Gerson, A., Thomas, J., Sobieraj, H., Schumann, R., Weisener, C., Weber, P., Miller, S., Stewart, W., 2002. ARD Testbook. Project P387A Prediction and Kinetic Control of Acid Mine Drainage. AMIRA International, Melbourne.
Soltani, N., Moore, F., Keshavarzi, B., 2013. Geochemistry of trace metals and rare earth elements in stream water, stream sediments and acid mine drainage from Darrehzar copper mine, Kerman, Iran. Exposure and Health 6, 97–114.
Watson, E.B., Chemiak, D.J., Hanchar, J.M., Harrison,TM., Wark, D.A., 1997. The incorporation of Pb into zircon. Chem. Geol. 141, 19–31.
WHO, 2004. World Health Organization. Guidelines for Drinking - Water Quality, third ed., vol. 1. recommendations, Geneva.
Zappettini, E.O., 1990. Mineralizaciones polimetálicas de los distritos El Queva, La Poma-Incacchule y Concordia, Salta. In: Zappettini, E.O. (Ed.), Recursos minerales de la República Argentina. Instituto de Geología y Recursos Minerales. SEGEMAR, Argentina, pp. 1603–1611.